

Better Bag Cleaning



Prof. Carlo Osnaghi,
Politecnico di Milano,
and Matteo Giavazzi,
Boldrocchi s.r.l., Italy,
provide their results
from a study on how
to improve efficiency
and reduce costs
through air jet bag filter
cleaning optimisation.

Abstract

In the filtration process, the dust transported by combustion gas is arrested on the bags' external surface, forming the so-called "cake". The dust cake builds up while the filtration process continues, with a speed depending on dust quantity, dust characteristics and air/cloth ratio. Bag filter pressure drop consequently increases and gas flow decreases with dust cake thickness.

Optimal gas distribution and an efficient preseparation upstream of the bag chambers reduce the speed of the dust cake build up. Nevertheless, the dust cake must be removed to prevent the increase in pressure drop, leading the bags to their original permeability.

Dust cake removal is obtained by means of a shock wave travelling along the bag, which accelerates the cloth outward until the bag is blocked by its own rigidity, while the dust cake detaches because of its inertia and falls down into the hopper (Figure 1).

The shock wave is generated by an injection of compressed air inside the bags, using nozzles placed at the entrance of each bag.

The cleaning frequency (number of shock waves for time unit) depends on the required pressure drop level and the cake build-up speed. For a required cleaning frequency, it is important to reduce energy consumption by optimising the design of the cleaning system, thus minimising the amount of compressed air used to create the shock wave inside the bags. At the same time, complex configurations of the secondary ejector must be avoided because they do not bring real advantages in terms of energy consumption or system efficacy.

The purpose of this article is to analyse different solutions for the geometry of the primary nozzle, secondary ejector and Venturi system in order to define the best solution in terms of system simplicity and energy saving.

Problem definition and scope of the survey

Different configurations of the geometry of the cleaning system (primary nozzle, secondary ejector, Venturi system) have been investigated, but not with the aim of measuring the absolute value of all the parameters involved in the process (in some cases the hypothesis necessary to model the phenomena has a negative influence on the precision of the results). Rather, the aim was to define, by means of comparisons among the measured values in different configurations, the configuration that allows minimum energy consumption with the simplest system configuration and best cleaning efficiency.

In particular, the ratio between the total amount of air (G_4) entering the bag (in order to generate a shock wave) and primary air coming from the compressed air generation system (G_1) must be as great as possible; that means one has to increase the total amount of air entering the bag, thus increasing the secondary air coming from external sources (filter chamber) and

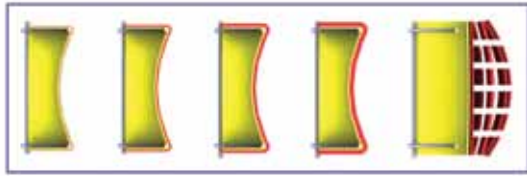


Figure 1. Dust cake detaches and falls into the hopper.

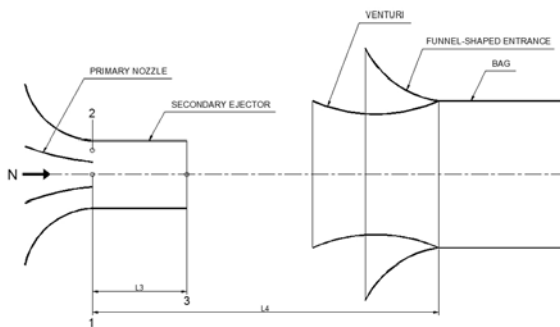


Figure 2. Geometry of the system.

Table 1. Glossary of parameters	
Parameter	Meaning
G	Amount of air (G_1 = compressed air generation system, G_4 = bag inlet)
D	Diameter (D_1 = primary nozzle outlet, D_3 = secondary ejector, D_4 = bag effective)
L	Distance of every section from primary nozzle (L_3 = secondary ejector, L_4 = bag)
P	Pressure in different sections
S	Surface of different sections
T	Temperature at different sections
U_m	Axial speed
r	Radial distance from the axis of the jet

reducing compressed air coming from the compressor, saving energy.

In fact, because of its viscosity, the high velocity air drags the surrounding gas into the bag neck (at the bag inlet).

The pressure and temperature at the nozzle can be fixed with the following geometry:

- Primary nozzle outlet diameter $D_1 = 11.5$ mm.
- Effective diameter of the bag $D_4 = 142$ mm.

Therefore, the mass flow at the nozzle becomes $G_1 = 145$ g/s.

The following parameters have been analysed in order to achieve a maximum value of G_4/G_1 :

- Distance between outlet section of the primary air jet and entrance of the bag L_4 .
- Presence of a funnel-shaped entrance at the bag inlet.
- Presence of a “Venturi” shaped entrance at the bag inlet and an eventual holes system in the Venturi’s neck.
- Presence of a secondary cylindrical ejector duct, fed by the primary nozzle in axis with the secondary, with different diameter D_3 and length L_3 .
- Substitution of the primary nozzle with one of the same section, but with an annular shape, in order to improve the contact surface between jet and ambient air.

The problem has been analysed with three different approaches:

1. With simplified software, specifically written in order to model the flow theory of ejectors.
2. With bi-dimensional CDF simulations (Fluent code).
3. By means of laboratory measures.

Simplified analytical models

This approach has been used to study the different behaviour of a simple nozzle in respect to an adapted nozzle and secondary ejector.

Flow theory of ejectors

Simple nozzle

Thanks to the theory of ideal flows in quasi-one-dimensional ducts, to obtain maximum mass flow the air speed in the outlet section of the nozzle must be sonic (same as the speed of sound, $Ma = 1$) and the pressure $P_1 = 0.528 P_0$.

Mass flow at the nozzle outlet can be calculated with the following formula (a glossary of the parameters used in the equations can be found in Table 1):

$$G_1 = \frac{p_0 \cdot S_1}{\sqrt{R \cdot T_0}} \cdot f(\gamma)$$

Where f = known function,
 R (air constant) = 287 J/kg*K,
 $\gamma = c_p/c_v = 1.4$.

With the given data the mass flow, as mentioned previously, results in $G_1 = 145$ g/s, the static pressure at the nozzle outlet $P_1 = 3.17$ bar and Ma (Mach number) = 1.

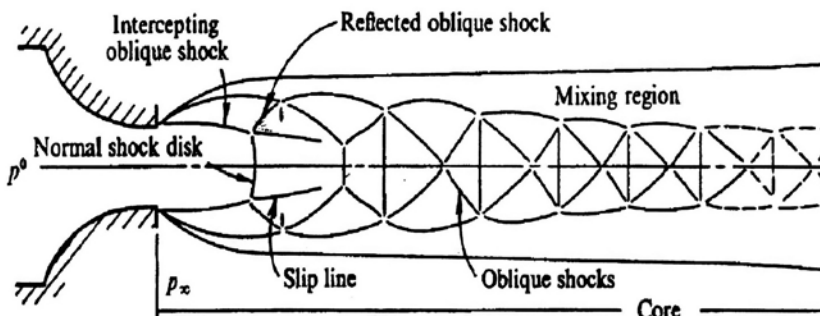


Figure 3. Air behaviour downstream of the nozzle: Near Field.

Downstream of section 1, mass flow expands in a complex way (in the zone called Near Field) and then assumes a pattern dominated by internal dissipation in the air jet and at the border with stationary air (this region is called Far Field).

In the Near Field, close to the nozzle outlet, there is a series of sharp expansions (Figure 3), followed by compressions through shock waves (diamonds and disks configuration).

Due to the great dissipation, this phenomenon ends after a length of 20 – 30 dia. and then starts the second region (Far Field) where the flow is completely developed. In this area the radius variation of the axial speed is “self-similar” (it is no longer influenced by the distance from the nozzle and then remains the same) and approximately representable with a Gaussian distribution (Figure 4).

Air jet axial speed, U_m , dimensionless among nozzle outlet speed $U_j = U_1$, decreases with the following exponential law:

$$\frac{U_m}{U_j} = 1 - e^{-\frac{1}{Q-Xc}}$$

With Q abscissa dimensionless among the nozzle diameter D_j and X_c among the core, which is the Near Field.

This formula is valid for $X/D_j > 10$, where X indicates the length of the core.

This equation expresses the speed distribution in every reference system and/or units (because the speed is dimensionless so it does not depend on the units used) and among an abscissa that considers both the dimension of the nozzle and the distance necessary for the complete development of the flow.

To calculate the mass flow one needs to know the speed distribution and the air density in the different transverse sections to the flow and distances from the nozzle.

Knowing axial speed U_m , the speed radial distribution can be described analytically by means of a Gaussian for $X/D > 10$:

$$\frac{U(r)}{U_m} = e^{-\ln 2 \left(\frac{r}{r_5}\right)^2}$$

Where r_5 indicates the radial distance from the axis of the air jet where the speed U is half of axial speed U_m .

Its value for a completely developed flow has been obtained by empirical evidences and it is valid both for supersonic and subsonic air jets:

$$r_5 = 0.0086 x$$

Supposing the density in the Far Field is uniform and the same for the ambient air, it is possible to calculate the mass flow of the air jet through integration.

Adapted nozzle

It can be interesting to analyse the case of an “adapted” nozzle, dimensioned to have a complete expansion up to ambient pressure at the outlet.

This requires a convergent-divergent duct with a well-dimensioned outlet section.

In this case, with the same neck section of 11.5 mm (so the same mass flow), the final diameter must be $D_1 = 13.94$ mm and Mach number $M_1 = 1.82$.

For the axial speed calculation the previous equations can be used.

‘Entrainment’ models

For the calculation of the mass flow in the Far Field, it is possible to integrate the speeds distribution or to use semi-empirical formulas.

For $X/D_1 \gg 1$

For subsonic or supersonic adapted air jets, calm external air, high Reynolds numbers, the mass flow G through the generic section X can be calculated with the following formula:

$$\frac{G}{G_1} = 0,32 \cdot \frac{X}{D_1} \cdot \left(\frac{\rho_1}{\rho_a}\right)^{1/2}$$

Where the ratio between parenthesis considers the different nature of outgoing and ambient fluid.

In case of sub-expanded nozzles (so called if the outgoing air pressure is higher than ambient air) it is possible to consider the overpressure on the nozzle section, multiplying the mass flow calculated before for a factor $(1+\Lambda)$, where $\Lambda=(F/M1)=(p_1-p_a)S$ (momentum at the nozzle outlet).

For $0 < X/D_1 < 12$

Boguslawski and Popiel suggest the following linear relation for the flow dragged G_E :

$$\frac{G_E}{G_1} = 0,183 \cdot \frac{X}{D_1}$$

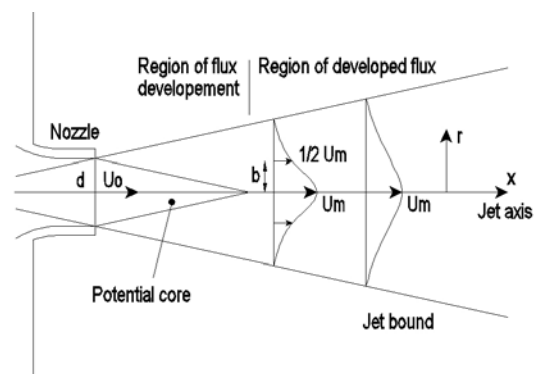


Figure 4. Air behaviour downstream of the nozzle: Far Field.

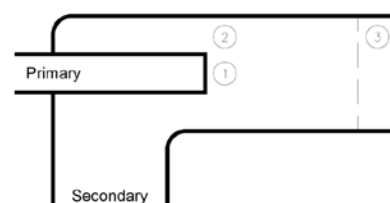


Figure 5. Sketch of the ejector.

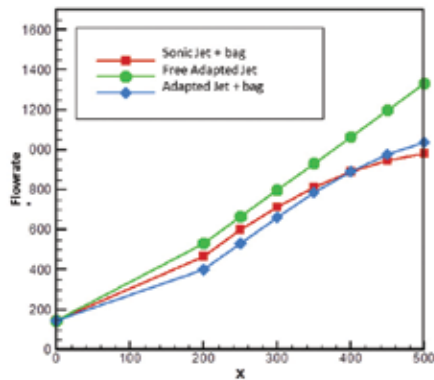


Figure 6. Mass flow rate [g/s] with different nozzles.

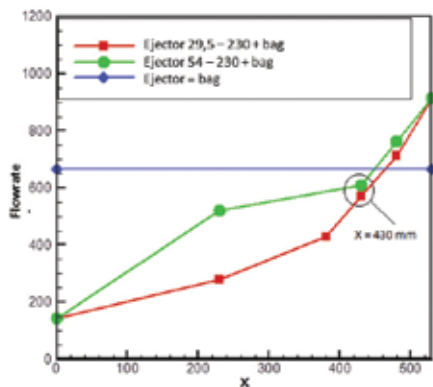


Figure 7. Mass flow rate [g/s] with secondary ejectors.

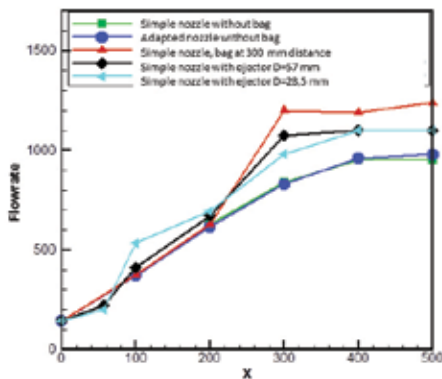


Figure 8. Mass flow rate [g/s] resulting from CFD calculation.

Ejector

The ejector consists of a system where a low energy flow (secondary) is energised by a high-energy air jet (primary).

It is a system that permits the increase of the secondary flow's energy in an easy way and without using any mechanical elements. It takes the energy of the primary flow, thanks to a mechanism of viscous dragging at the board of the jets, and substantially increases the flow downstream of the ejector compared with the primary flow.

Obviously the efficiency of this process is extremely low.

The optimisation of the geometry is a complex problem, but it is possible to reduce it to a very simple equation using some simplifications:

- Assuming the secondary duct downstream of section (2) in Figure 5 is cylindrical.
- Assuming the secondary duct is long enough to permit the complete mixing of the two flows at the outlet (uniform flow in section (3)). This requires a length of 20 – 30 dia. of the primary.
- Neglecting viscous efforts on the side of the secondary.

The ejector's objective, for this purpose, is to maximise secondary flow by means of the primary jet, so the total flow in (3), acting on the only parameter available, is the ratio of the sections S_1/S_3 , with an adequate length of the secondary.

System ejector – free air jet

The objective of maximising the ingoing flow in the bag (i.e. the ratio G_4/G_1) can also be reached with a mixed solution: first flow is increased compared to the primary jet, through an ejector; an "entrainment" in free jet downstream, starting from the flow outgoing the ejector, is presumed mixed and so uniform.

This is a low energy jet, being generated by means of a viscous mixing, so the next "entrainment" is lower than the one obtainable with a first jet in free atmosphere.

It is necessary to examine the different intermediate situations between the two extremes, that are: 1) no ejector and 2) nozzle at the entrance of the bag. (In this case, the bag itself will become a kind of secondary duct, even if a very particular one, because the outlet section would be the cylindrical side, while the end section would be closed.)

Results of simplified models

Simple nozzle

The results of the calculations are listed for different distances from the nozzle in the following cases (Figure 6, representing mass flow rate as a function of distance):

- Free jet with adapted nozzle (green). In this case, the mass flow in the chosen section is extended up to an infinite radius.

TALK TO US –
OUR SERVICE IS YOUR SUCCESS!



Phone: +49 8121 707-0
Web: www.rema-tiptop.com

THE PERFECT WAY
TO RUN YOUR OPERATION.



- Free jet with adapted nozzle (light blue), integrated up to $r = 71$ mm (bag radius).
- Free jet with convergent sub expanded nozzle (red), integrated up to $r = 71$ mm.

It is possible to note that:

- The increase in flow is already high for distances around 300 mm ($G_4/G_1=5$).
- The comparison between jet in free air and jet with the presence of the bag shows that, in this last situation, the flow is lower and, after a certain distance, it tends to saturate and it reaches a maximum (not represented in the figure).
- The comparison between convergent and adapted nozzle shows that there is no gain with this second disposition and so it is preferred to operate with the cheaper and simpler convergent nozzles.

Ejector and free subsonic air jet

The following system has been simulated using calculation software: primary nozzle, secondary ejector (cylindrical pipe with theoretical infinite length), and bag.

In the calculation, the length of the ejector has been assumed as $L_3 = 230$ mm, in order to define the length of free jet downstream of the ejector, measuring $L_4 - L_3$.

Three cases have been considered (Figure 7):

1. Ejector: $D_3 = 29.5$ mm, $L_3 = 230$ mm.
2. Ejector: $D_3 = 54$ mm, $L_3 = 230$ mm.
3. Ejector: $D_3 = D_4 = 142$ mm, $L_3 = L_{bag}$.

As the distance $x = 230$ mm represents section 3 (outlet of ejector), the smaller ejector achieves less flow rate compared to the bigger, but the jet at the outlet is faster, so the following entrainment is higher. At 200 mm downstream ($x = 430$ mm), the flow rates with the two ejectors are already identical, but are both less than the one obtained without ejector (shown in Figure 6).

CFD simulations

Problem definition

In order to validate the results obtained with analytical models, the system has been modelled using computational fluid dynamic tools.

The following cases have been simulated:

- Simple nozzle without bag (green line).
- Adapted nozzle (convergent – divergent) without bag (blue line).
- Simple nozzle, bag at 300 mm distance (red line).

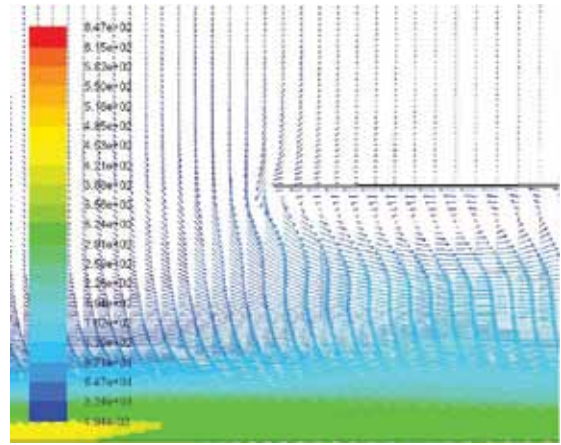


Figure 9. Air speed [m/s] at bag inlet.

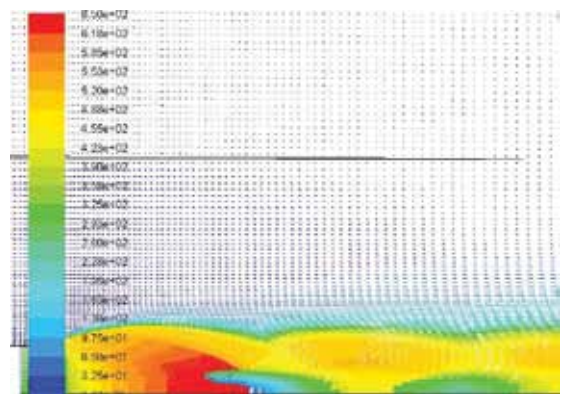


Figure 10. Air speed [m/s] at ejector outlet.



Figure 11. Test equipment.

The **REMA TIP TOP** service team supports you quickly and expertly wherever you are.

A powerful portfolio of services and effective teamwork – that is why **REMA TIP TOP** sets the standards in service. Our comprehensive portfolio ranges from analyzing your needs and planning a solution to fit them, supplying logistics and construction work, and takes in training, maintenance and repair. Our service network, operating throughout the world, supports your onsite activities immediately. We deliver all you need – quickly, expertly and flexibly. So take advantage of the powerful **REMA TIP TOP** service concept now.



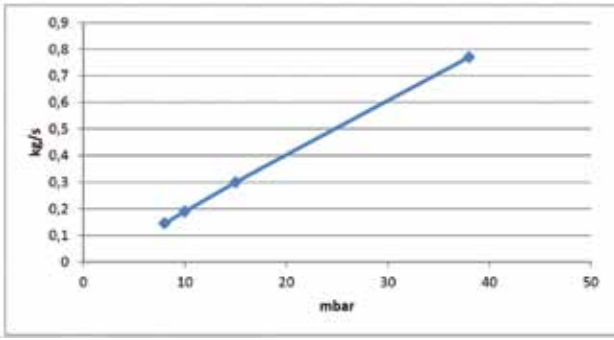


Figure 12. Correlation curve between pressure and flow rate inside bag.

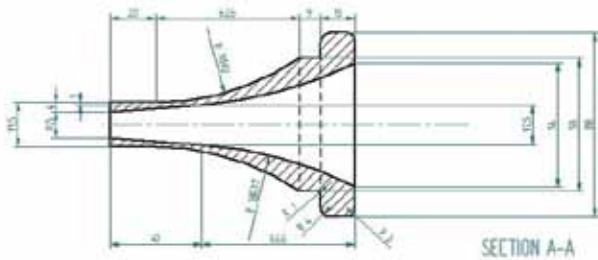


Figure 13. Simple nozzle.

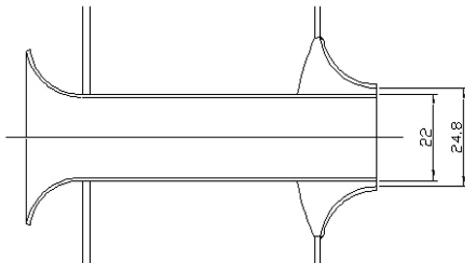


Figure 14. Annular nozzle.



Figure 15. Ejector test.

- Simple nozzle with ejector ($D_3=57$ mm, $L_3=57$ mm), bag at 300 mm distance (black line).
- Simple nozzle with ejector ($D_3=28.5$ mm, $L_3=57$ mm), bag at 300 mm distance (light blue line).

The calculations have been performed under the following hypothesis:

- Turbulence model $k-\omega$ SS with $\gamma+=1$.
- Total pressure and temperature assigned upstream of the nozzle.
- The border of the external domain of the nozzle and the bag (atmosphere) is situated far enough away: upstream and laterally it is assumed as inlet surface with total atmospheric pressure, downstream it is possible to have an inlet and outlet flow in atmospheric condition.
- The bag is considered impermeable, but is open downstream where atmospheric pressure is imposed.
- An extremely tight grid was used for the calculation, because the problem is dominated by the viscous dragging at the borders of the primary and the secondary jet. A grid with 50 000 nodes was used.
- An aggregate calculation (based on density) was used that was particularly suitable for the region of the primary air jet, extremely compressible, but not good for the external area where velocities are very low and the air is incompressible.

CFD calculation results

Figure 8 describes the results of CFD calculation (mass flow rate in g/s as a function of distance).

It can be noted that:

- The numerical values are in accordance with the ones resulting from the theory of flow ejectors.
- It is confirmed that adapted nozzles (convergent – divergent) do not allow relevant advantages in terms of increasing flow rate.
- The presence of a bag increases the flow rate, as it behaves as an ejector, taking in external air (Figure 9).
- In terms of global flow rate increasing, it is confirmed that the ejector is not favourable, especially if its length is limited and does not allow complete mixing (Figure 10).



Figure 16. Venturi at bag inlet – holes system for air entrance.

Figure 9 shows the field of speed vectors at the entrance of the bag; it is evident that the air intake is relevant.

Figure 10 shows the field of speed vectors in the area at the ejector outlet $D_3 = 28.5$ mm; the flux is not mixed.

Laboratory measures

Tests have been performed inside Energy Department of Politecnico of Milan using certified regulation devices and measuring sensors.

Problem definition

Figure 11 shows the system used for laboratory tests: in particular the bag and the compressed air tank. A bag with modified permeability has been used, in order to simulate real conditions of the bag with dust cake on its surface.

In order to measure the flow rate of compressed air inside the bag, static pressure sensors have been placed on bags, after having obtained the correlation curve between pressure and flow rate (Figure 12).

Using this curve, compressed air flow rate has been calculated for each condition starting from the mean values of static pressure on the bag surface.

Nozzle types

Different types of nozzles have been tested, both simple and modified, in order to increase the surface between the compressed air jet and external air, and consequently the air entrainment.

Simple nozzles have an outlet diameter of 11.5 mm (Figure 13), while modified convergent-divergent nozzles have the same neck diameter and an outlet diameter of 13.98 mm.

An annular nozzle, with the same area as the simple nozzle, is shown in Figure 14. In this nozzle the compressed air jet's internal and external surface is in contact with external air.

Ejectors

Two types of ejectors have been tested, with diameters D_3 of 28.5 and 54 mm, both 230 mm long (Figure 15).

Venturi system at bag inlet

Both simple funnel-shaped or Venturi systems have been tested and modified in order to maximise external air entrance by means of a multi-hole system.

A venturi inlet section has been placed at a distance $L_4 = 200$ mm from the nozzle (Figure 16).

Results from laboratory measures

Figure 17 shows air flow with simple nozzle (red and green), nozzle and Venturi (light blue), and annular nozzle and Venturi (black).

It is evident that the annular nozzle, after a distance, gives an increase in air flow rate, but not so significant as to justify the complexity and cost of its installation.

The best results come from the simple nozzle with multi-hole Venturi system (light blue).

From Figure 18 it is possible to understand that an ejector without Venturi system is not effective (red and black lines); a significant increase in air flow rate is obtained only with this latter (green and light blue lines).

A simple funnel-shaped entrance is also not effective.

The same conclusions come from Figure 19, referring to a smaller diameter ejector. The green line refers to a Venturi

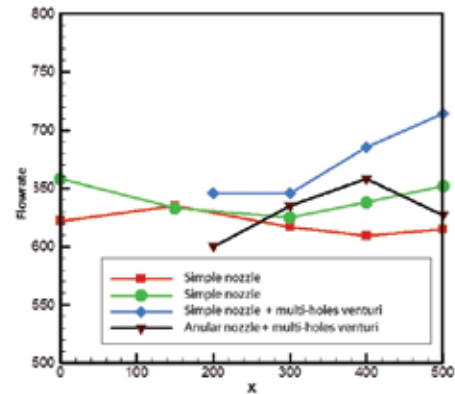


Figure 17. Comparison of mass flow rates [g/s] in laboratory tests.

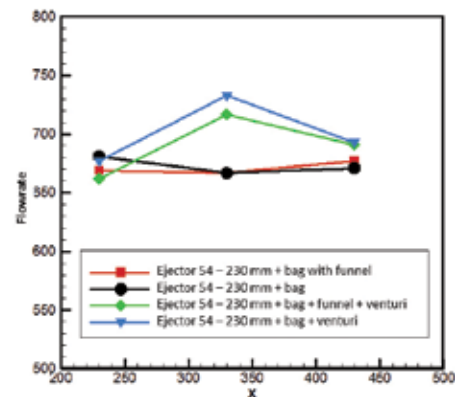


Figure 18. Direct comparison of flow rate with or without Venturi with multi-holes.

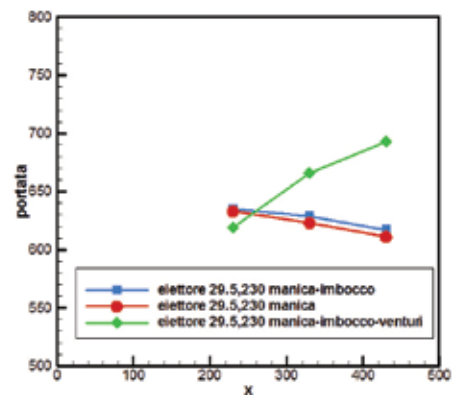


Figure 19. Direct comparison of flow rate with or without Venturi with multi-holes.

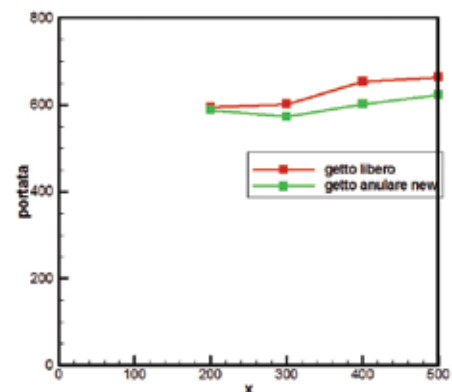


Figure 20. Comparison between simple nozzle and an annular one.



Explosion protection for industries typically using coal lignite, pet coke and secondary fuels

Thorwesten Vent are your experts in explosion venting and pressure shock resistant design and construction. Thorwesten Vent offers explosion protection-related consultancy for the planning of new as well as the correction of existing grinding facilities for solid fuels. We provide for your safety!

- Highly efficient self-reclosing explosion vents
- Customized safety solutions comprising engineering and hardware supply
- Professional consulting and assistance



We provide for your safety

THORWESTEN VENT

THORWESTEN VENT GmbH
Daimlerring 39 · 59269 Beckum / Germany
Phone. +49(0)2521/9391-0
thorwesten.vent@thorwesten.com
www.thorwesten.com

system, which always performs better and ensures greater air to the bag.

Figure 20 shows a direct comparison between a simple nozzle (red) and an annular one (green), confirming the simple nozzle is the best choice. An annular nozzle supplies mass flow rates very similar to the one referred to as a simple nozzle, but it is more complicated and expensive.

Conclusion

In order to achieve maximum efficiency in bag cleaning, the aim is to generate a pressure wave inside the bag using the minimum quantity of primary compressed air, in order to save as much energy as possible.

Under the hypothesis of the current analysis, it is not demonstrated that either a complicated primary nozzle, or an ejector system is needed.

In this latter case, the compressed air flow increase is evident with ejector diameter of 57 mm, but the speed at the outlet is consequently reduced, so that the downstream entrainment decreases. As a consequence, the total effect remains unchanged, without great energy consumption reduction or efficiency increasing.

On the contrary, the contribution of the Venturi system at the bag entrance is remarkable, and further maximised with an optimal holes distribution system from which further external air is taken in.

The cumulative effect of the simplest and best performing cleaning system geometry, with an expert cleaning control board and optimised algorithms to control filter differential pressure setpoint, allows maximum cleaning efficiency and minimum energy consumption. 🌐

Bibliography

- BALL, G. and POLLARD, A., *A review of experimental and computational studies of flow from the round jet.*
- BOGUSLAWSKI, L. and POPIEL, O., *Flow structure of the free round turbulent jet in the initial region* (1978).
- EWAN, B.C.R. and MOODIE, K., *Structure and Velocity Measurements in Underexpanded Jets* (1985).
- HUANG, B.J. and CHANG, J.M., *A 1-D analysis of ejector performance.*
- KENTFIELD, J.A.C. and BARNES, R.W., *The prediction of the optimum performance of ejectors.*
- PAPADOPULOS, G. and PITTS, W., *Scaling the near-field centerline mixing behavior of axisymmetric turbulent jets.*
- UEBELHACK, H.T., *One-dimensional inviscid analysis of supersonic ejectors.*

The authors

Carlo Osnaghi has been Professor in "Turbomachinery" at the Politecnico di Milano since 1969. Throughout his career he has carried out intense numerical and experimental research activity in the field of energy and power plants, notably in the turbomachinery area.

Matteo Giavazzi is an Environmental Engineer with 15-years experience in industrial plants process engineering. He is a specialist in air quality, pollution prevention and environmental problems analysis, with particular reference to air pollution from industrial sources.